Journal of Organometallic Chemistry, 452 (1993) 185–192

JOM 23336

$[Co_4(CO)_{12}]$ derivatives with bis(diphenylphosphino)amine, an electrochemical study

C. Moreno, M.J. Macazaga, M.L. Marcos, J. González-Velasco and S. Delgado

Departamento de Química, Universidad Autónoma de Madrid, Cantoblanco, 28049 Madrid (Spain)

(Received July 16, 1992)

Abstract

$[Co_4(CO)_{12}]$ (**A**) reacts with bis(diphenylphosphino)amine (dppa) to give $[Co_4(CO)_{10}(dppa)]$ (**B**) or $[Co_4(CO)_8(dppa)_2]$ (**C**) when the reactant ratios are 1:1 or 1:2, respectively. The complexes have been characterized by elemental analysis, IR, ^1H and ^{31}P NMR spectroscopy. The electrochemical behaviour of the three compounds has been studied. The reduction voltammetric waves and the first oxidation of C are reversible, although other waves were also observed which were attributed to the fragmentation induced by electron transfer. Using the electrochemical and UV-visible data, it was possible to construct MO diagrams and to locate the HOMO, LUMO and other MOs of the metal core.

1. Introduction

Ligand-substitution processes in cluster complexes, especially in tetranuclear clusters such as $[Co_4(CO)_{12}]$ have been of great interest in recent years. It has been consistently demonstrated that replacement of carbon monoxide is an important feature in such reactions [1–7]. However, polydentate phosphines may stabilize the cluster against fragmentation. Thus the tripod ligand $HC(PPh_2)_3$ stabilizes the cluster series $[M_4(CO)_9\{HC(PPh_2)_3\}]$ (M = CO, Rh, or Ir) towards fragmentation, allowing comparative mechanistic studies of ligand effects on the substitution labilities with a variety of phosphorus donor ligands [8]. The clusters $[Co_4(CO)_8(dppm)_2]$ (dppm = bis(diphenylphosphino)methane) [9], $[Co_4(CO)_9(dpmp)]$ and $[Co_4(CO)_7(dpmp)_2]$ (dpmp = bis(diphenylphosphino)methylphenylphosphine) [10] are also stable.

Electrochemical studies on $[Co_4(CO)_{12}]$ and some phosphine derivatives confirmed the importance of CO lability in substitution reactions [11,12] and the stability of electrogenerated cluster monoanion radicals was enhanced when bis- or tris-phosphine capping moieties were bound to the cluster [13,14].

We report here an investigation of the substitution reactions of $[Co_4(CO)_{12}]$ with dppa (bis(diphenylphosphino)amine), and an electrochemical study of the isolated complexes.

2. Results and discussion

Addition under N_2 of a dichloroethane (DCE) solution of dppa to a solution of $[Co_4(CO)_{12}]$ (**A**) in the same solvent resulted in loss of CO to give $[Co_4(CO)_{10}(dppa)]$ (**B**) or $[Co_4(CO)_8(dppa)_2]$ (**C**) when the reactant ratios were 1:1 or 1:2, respectively. The compounds were characterized by elemental analysis and IR, ^1H and ^{31}P NMR spectroscopy. Table 1 lists the carbonyl stretching frequencies of the substituted products.

The complex $[Co_4(CO)_{10}(dppa)]$ shows seven bands between 2070 and 1930 cm^{-1}, and three bands in the 1860–1770 cm^{-1} range, arising from terminal and bridge ligands. This is consistent with a C_s molecular symmetry. The spectrum is similar to that of $[Co_4(CO)_{10}(P(OMe)_3)_2]$ whose structure is known [15], suggesting a similar structure with two axial carbonyl groups in the basal plane of cobalt atoms replaced by the dppa molecule as shown in **I**.

The IR spectrum of $[Co_4(CO)_8(dppa)_2]$ is also consistent with C_s molecular symmetry: five bands in the 2010–1930 cm^{-1} range and three between 1830 and

Correspondence to: Professor S. Delgado.

0022-328X/93/$6.00

1770 cm^{-1} attributable to terminal and bridge ν(CO) vibrations, respectively. The highest ν(CO) absorption band (2010 cm^{-1}) falls in the range characteristic of tetrasubstituted derivatives [13,16]. The similarity of this spectrum with that of [Rh$_4$(CO)$_8$(dppm)$_2$] [17] suggests a structure where both dppa ligands bridge two cobalt atoms as indicated in **II**.

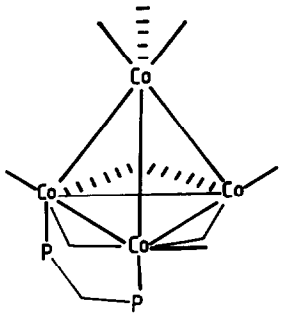

I

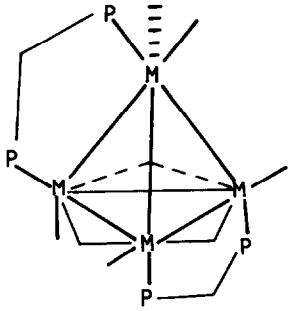

II

In both compounds, the band corresponding to ν(P–C) appears at 695 cm^{-1}, and ν(N–H) at 3300 cm^{-1} is shifted, as usual, towards higher energies relative to that of the free donor (3225 cm^{-1}) [18].

The ^{1}H and ^{31}P NMR data are reported in the Experimental section. For both complexes, the ^{31}P NMR spectra consist of a singlet shifted significantly downfield due to the equivalence of the two P atoms.

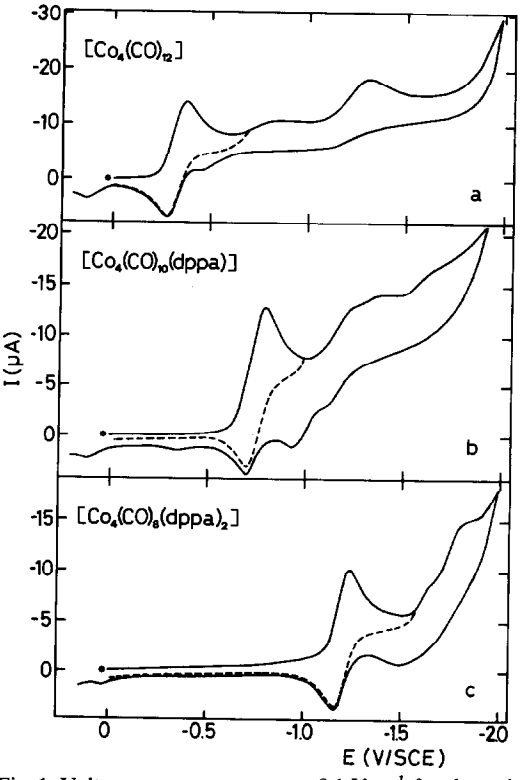

Fig. 1. Voltammograms run at $v = 0.1$ V s^{-1} for the reduction of the clusters. DCE + 0.1 M TBAP solution. $C_{cluster} = 5 \times 10^{-4}$ M. 25°C. (*) Start of cycle.

2.1. Electrochemical reduction

Cyclic voltammetry studies of the three cluster compounds in 1,2-dichloroethane solutions show a one-electron reduction step to the corresponding radical anion [Co$_4$(CO)$_{12-2n}$(dppa)$_n$]$^{\cdot-}$ (Fig. 1), which is elec-

TABLE 1. Carbonyl stretching frequencies (cm^{-1}) for the complexes

Co$_4$(CO)$_{10}$(dppa)		Assignment	Co$_4$(CO)$_8$(dppa)$_2$		Assignment	
a	b		a	b		
2068vs	2068s	A′	2005s	2010s	A′	
2029vs	2048m	A′	1972vs	1980vs	A′	
2005vs	2029s	A′	1965vs	1970vs	A″	ν(CO)$_t$
1972br,vs	2013vs	A″	1951sh	1948sh	A′	
1965br,vs	1989s	A′	1936s	1937sh	A″	
1949sh	1967sh	A′				
1938sh	1944sh	A″				
1841m	1859m	A′	1830m	1829m	A′	
1795s	1825s	A′	1796s	1790s	A′	ν(CO)$_b$
1778s	1793s	A″	1779s	1777s	A″	

[a] KBr plates. [b] DCE solution.

trochemically reversible (the increase in ΔE_p with the scan rate parallels that of the standard ferrocene/ferricenium couple under the same conditions). $E^{0\prime}$ values shift to more negative potentials as the degree of substitution by dppa ligands increases, *i.e.* $E^{0\prime}$ is −334 mV/SCE for **A**, −755 mV/SCE for **B** and −1205 mV/SCE for **C**. This reduction step is diffusion-controlled, as i_{pc} depends linearly on the square root of the scan rate in the range $0.01\ V\ s^{-1} < v < 0.5\ V\ s^{-1}$. On the other hand, $i_{pa}/i_{pc} < 1$ in the same range of scan rate, which indicates that the reduced form of the compound participates in a chemical reaction in homogeneous solution. More data are assembled in Table 2.

The diffusion coefficients of the cluster compounds, **D**, are related to i_{pc} at 25°C as shown in eqn. (1) [19]

$$i_{pc} = 2.69 \times 10^5 n^{3/2} A D^{1/2} v^{1/2} C \quad (1)$$

where A is the real surface area of the electrode and C is the bulk concentration of the oxidant cluster compound. As shown in Table 2, i_{pc} decreases as dppa ligands replace CO in the clusters. Accordingly, D values decrease in the same way, as expected from the increasing radii of the compounds. From an analysis of i_{pc} at different sweep rates, D_A was found to be 0.43 $D_{ferrocene}$, $D_B = 0.8 D_A$, and $D_C = 0.7 D_B$. With the value of $D_{ferrocene}$ in DCE (1.06×10^{-5} cm^2 s^{-1}) calculated from literature data [20] and Walden's rule [21], the diffusion coefficients of the three clusters were obtained (see Table 2). These values are practically coincident with those resulting from direct application of eqn. (1).

When the cathodic sweep extends beyond the first reversible peak to −1.8 V/SCE with $[Co_4(CO)_{12}]$, two more irreversible reduction peaks appear, at −0.85 V and −1.32 V/SCE, as well as a new anodic peak at *ca.* −0.47 V. The last does not appear when the negative sweep limit is −0.7 V. With $[Co_4(CO)_{10}(dppa)]$, the cathodic scan extended until −1.8 V/SCE shows a further three less precisely defined peaks at −1.24 V, −1.34 V and −1.65 V/SCE. The first seems to have a

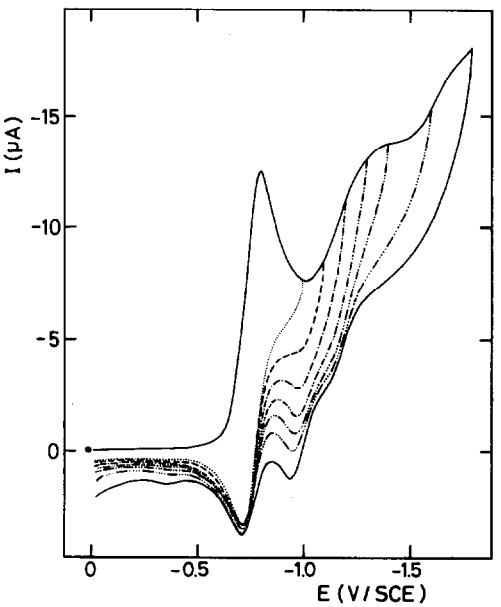

Fig. 2. Voltammograms run at 0.1 V s^{-1}. Solution of $Co_4(CO)_{10}(dppa)$ (5×10^{-4} M) in DCE+0.1 M TBAP. (*) Start of cycle. Negative potential limit: −1 V (·····); −1.1 V (— — —); −1.2 V (-·-·-); −1.3 V (-··-··-); −1.4 V (-···-); −1.6 V (-·····-); −1.8 V (———).

corresponding oxidation at −1.14 V. At the same time, the anodic sweep shows the appearance of two new peaks, at −0.94 V and −0.39 V/SCE, whose dependence on the cathodic potential limit is shown in Fig. 2. If the anodic scan under these conditions extends beyond 0 V, a peak at +0.1 V can be observed for clusters **A** and **B**. An examination of the existing literature [22] suggests that it is due to the oxidation of $[Co(CO)_4]^-$ produced by cluster fragmentation to the radical $[Co(CO)_4]$.

When $[Co_4(CO)_8(dppa)_2]$ is in solution and the potential is swept beyond −1.6 V, a new reduction peak appears at −1.85 V, as well as an oxidation peak at −1.55 V on the positive potential scan. This wave is probably due to a second reduction of the cluster,

TABLE 2. Electrochemical results: Pt working electrode; $C_{cluster} = 5 \times 10^{-4}$ M; DCE + 0.1 M TBAP; 25°C; all potential values referred to SCE ($E^{0\prime}$(ferrocene/ferricenium) = +0.495 V/SCE)

Compound	First reduction				Oxidation				D (cm^2 s^{-1})
	$E^{0\prime}$ [a] (mV)	E_{pc} [b] (mV)	E_{pa} [b] (mV)	i_{pc} [b] (μA)	$E^{0\prime}$ (mV)	E_{pa} [b] (mV)	E_{pc} [b] (mV)	i_{pa} [b] (μA)	
$Co_4(CO)_{12}$	−334	−375	−282	14.2	1385 [c,d]	1450 [d]	–	90	4.7×10^{-6}
$Co_4(CO)_{10}(dppa)$	−755	−797	−707	12.7	1000 [c]	1055	–	65	3.8×10^{-6}
$Co_4(CO)_8(dppa)_2$	−1205	−1240	−1165	10.4	475 [a]	520	435	12.1	2.7×10^{-6}

[a] Taken as the average value of $(E_{pa} + E_{pc})/2$ for the different sweep rates studied. [b] Data obtained at $v = 0.1$ V s^{-1}. [c] Irreversible wave, taken as the potential at $i = 0.8 i_{pa}$. [d] This is the highest intensity oxidation peak. There is another peak at +1050 mV whose intensity grows with time (see text).

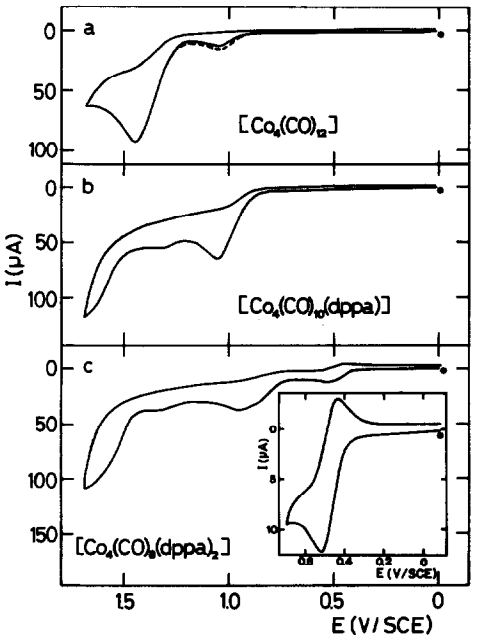

Fig. 3. Voltammograms run at $v = 0.1$ V s^{-1} for the oxidation of the clusters. DCE+0.1 M TBAP solution. $C_{cluster} = 5 \times 10^{-4}$ M. 25°C. (*) Start of cycle. (— — —) Voltammogram run 5 min after the first one represented by the solid line.

generating $[Co_4(CO)_8(dppa)_2]^{2-}$. An oxidation of $[Co(CO)_4]^-$ to $[Co(CO)_4]^{\cdot}$ can also be observed, but the corresponding peak is of a much smaller intensity than that obtained for compounds **A** and **B**. We tried to measure the amount of $[Co(CO)_4]^-$ produced by cluster fragmentation by recording IR spectra of electrolysis solution samples. While the band at 1890 cm^{-1}, [due to $Co(CO)_4^-$], was clear for **A** and **B**, this was not the case with **C**.

These results indicate that, for cluster **C**, fragmentation does not play such an important role, and the anion radical $[Co_4(CO)_8(dppa)_2]^{\cdot -}$ is more stable than $[Co_4(CO)_{12}]^{\cdot -}$ or $[Co_4(CO)_{10}(dppa)]^{\cdot -}$. This trend is in agreement with results found on related compounds in which polydentate phosphine ligands stabilize the cluster against fragmentation [22].

2.2. Electrochemical oxidation

$[Co_4(CO)_{12}]$ and $[Co_4(CO)_{10}(dppa)]$ exhibit irreversible oxidation peaks (see Fig. 3 and Table 2) of very high intensity, indicating multi-electron processes. The voltammogram corresponding to $[Co_4(CO)_{12}]$ also features a clear oxidation peak at +1.05 V/SCE, which grows slightly with the time of contact between electrode and solution. A similar peak does not appear with the dppa-substituted compounds.

The voltammogram for $[Co_4(CO)_8(dppa)_2]$ features a reversible one-electron oxidation at $E^{0\prime} = +0.478$ V/SCE. The process is diffusion-controlled (i_{pa} depends linearly on $v^{1/2}$ for 0.02 V s$^{-1} < v < 0.4$ V s^{-1}). Beyond this peak, irreversible multi-electron oxidations take place at $E_p = +0.97$ V and +1.34 V/SCE. Once more, the stabilizing effect of the phosphine is evident.

2.3. Electrochemical study of substitution of CO by dppa ligands

The characteristics of the first reduction peak for the three clusters make it possible to follow voltammetrically the kinetics of the substitution of CO by dppa. This technique might also show the presence of intermediate mono or tri *P*-substituted clusters, provided these species have a long enough lifetime. For these purposes, voltammograms at a high sweep rate (0.4 V s^{-1}, in order to minimize the influence of the potential scan on the reaction) were taken at different times, leaving the solution at open circuit between measurements. The substitution of two CO by dppa yielding $[Co_4(CO)_{10}(dppa)]$ is a very rapid process. Ten seconds after the addition of dppa to a solution of $[Co_4(CO)_{12}]$ in a 1:3 cluster-ligand ratio, most of this cluster has disappeared, as shown by the diminution of its reduction peak at $E_{pc} = -390$ mV. The presence of a peak at $E_{pc} = -790$ mV indicates a new substance, which should be cluster **B**. Forty-five seconds after the addition, $[Co_4(CO)_{12}]$ has completely disappeared, whilst the peak at −790 mV reaches its maximum i_p value.

Evidence for $[Co_4(CO)_8(dppa)_2]$ is a reduction peak at $E_{pc} = -1280$ mV, which appears 5 min after adding dppa to the initial solution. This second substitution of two CO by a further dppa is much slower than the first. Approximately one-third of $[Co_4(CO)_{10}(dppa)]$ is still present 3 h after the start of the experiment, as calculated from the height of the peak at −790 mV. At the same time, a new reversible wave (not observed in any of the potential sweeps applied to solutions containing the isolated complexes) appears in a potential range between those at which the di- and tetra-*P*-substituted compounds show a corresponding wave. This new wave is characterized by $E_{pc} \approx -1050$ mV and $E_{pa} \approx -950$ mV. Figure 4 shows the voltammogram taken at $v = 10$ mV s^{-1} obtained 4 h after the addition of dppa. At this sweep rate, the three reversible waves can be clearly observed. The new wave is attributed to an intermediate trisubstituted cluster $[Co_4(CO)_9(\eta^2\text{-dppa})(\eta^1\text{-dppa})]$.

To obtain a confirmation of the tricoordinated species, a ^{31}P NMR spectrum of a solution of $[Co_4(CO)_{12}]$ and dppa (1:3 ratio) in $CDCl_3$ was taken after 3 h of reaction. The spectrum showed a singlet at 62.2 ppm attributable to the coordinated P atom of the η^1-dppa ligand as reported in a previous paper [23]. Signals at 74.5 ppm (η^2-dppa) and 51.5 ppm (uncoordinated P of η^1-dppa) were also observed.

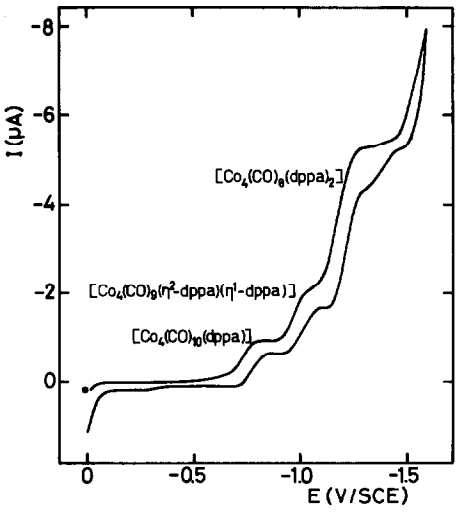

Fig. 4. Voltammogram run at $v = 0.01$ V s^{-1} obtained 4 h after the addition of dppa to a solution of compound **A** in a 1:3 cluster to ligand ratio. DCE + 0.1 M TBAP solution. (*) Start of cycle.

A similar electrochemical study was made with a 1:2 cluster/dppa ratio. All the substitution reactions were then slower. The initial peak at −390 mV corresponding to the reduction of **A** has very little intensity 45 s after the start of the experiment, although it does not completely disappear until 10 min later. Correspondingly, the reduction peak of **B** appears very soon and reaches its maximum intensity 10 min after the addition of dppa. However, the diminution in intensity of this peak is now very slow and after 2 h of reaction there is only a very small peak due to the reduction of **C**, which seems to indicate that at this temperature and reactant ratio the formation of **C** is a very slow process. The wave that we attributed to the trisubstituted intermediate cluster can also be observed, but not so clearly as when the cluster/dppa ratio was 1:3.

TABLE 3. Electronic absorption spectra data for band maxima in DCE solution

Compound	λ (nm)	cm^{-1}	eV
$Co_4(CO)_{12}$	560sh	17860	2.21
	470sh	21280	2.64
	376 ($\sigma \rightarrow \sigma^*$)	26600	3.30
$Co_4(CO)_{10}(dppa)$	510	19610	2.43
	378 ($\sigma \rightarrow \sigma^*$)	26450	3.28
$Co_4(CO)_8(dppa)_2$	596	16780	2.08
	528	18940	2.35
	440sh	22730	2.82
	380 ($\sigma \rightarrow \sigma^*$)	26320	3.26
	305	32790	4.06
	260	38460	4.77

2.4. *UV-visible spectroscopy*

UV-visible spectra of the three cluster compounds were taken in DCE solution (Table 3). In each case, the highest intensity band is around 380 nm and has been assigned to the $\sigma \rightarrow \sigma^*$ transition [24].

2.5. *Correlation between spectroscopic and electrochemical results*

The conservation of the main UV-visible spectral band at around 380 nm in the three clusters indicates that the $\sigma \rightarrow \sigma^*$ transition does not change as CO is replaced by dppa. On the other hand, the electrochemical results indicate that the first oxidations and the first reductions are separated by the same energy gap (see Table 4). We therefore postulate that the molecular orbitals involved in both the spectroscopic transition and in the electrochemical electron-transfers remain unchanged in form and energy. The only change detected could be the position of such a group of MOs in the energy scale. Figure 5 is a diagram of such orbitals, based on the calculations by Holland *et al.*

TABLE 4. Assignment of electrochemical and spectroscopic transitions; all potential values referred to SCE

	$Co_4(CO)_{12}$	$Co_4(CO)_{10}(dppa)$	$Co_4(CO)_8(dppa)_2$
$E^{0\prime}_{red}$ (mV)	−334	−755	−1205
Electrochemical transition	$(27e)^0 \rightarrow (27e)^1$	$(27e)^0 \rightarrow (27e)^1$	$(27e)^0 \rightarrow (27e)^1$
$E^{0\prime}_{ox}$ (mV)	1385	1000	475
Electrochemical transition	$(20a_1)^2 \rightarrow (20a_1)^1$	$(20a_1)^2 \rightarrow (20a_1)^1$	$(20a_1)^2 \rightarrow (20a_1)^1$
$E^{0\prime}_{ox} - E^{0\prime}_{red}$ (mV)	1719	1755	1680
λ ($\sigma \rightarrow \sigma^*$), nm (eV)	376 (3.30)	378 (3.28)	380 (3.26)
Spectroscopic transition	22e → 27e	22e → 27e	22e → 27e

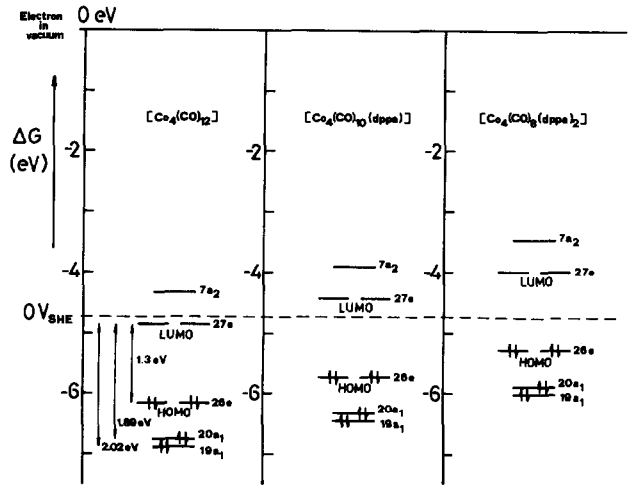

Fig. 5. MO diagrams of the three cluster compounds. Based on experimental data and calculations by Holland *et al.* [24].

[24]. The energy scale is referred to the physical energy zero, corresponding to the energy of an electron at infinity. This zero has been translated to the electrochemical energy scale based in the SHE which corresponds to -4.73 eV with respect to the physical energy scale [25]. The first reduction in each cluster is supposed to occur as a consequence of an electron transfer from the electrode to the LUMO of the cluster which can thus be placed on the energy scale. Once the LUMO is determined, the MO ensemble which supposedly remains unchanged is also located, as indicated in Fig. 5.

The LUMO is presumably the σ^* orbital to which the $\sigma \rightarrow \sigma^*$ metal centred absorption is assigned. It seems that the substitution of CO by dppa does not change the distance between the metal-centred molecular orbitals, but that these MOs are shifted towards more negative potentials on the energy scale. This is supported by the fact that both the separation between oxidation and reduction waves in the clusters and the main spectroscopic transitions remain unchanged for all three compounds. Substitution of two CO by one dppa shifts $E^{0\prime}_{red}$ by -421 mV (40.5 kJ). A second substitution of two CO by another dppa produces a $\Delta E^{0\prime}_{red} = -450$ mV, corresponding to an almost equivalent shift of the LUMO of **C** with respect to that of **B** on the energy scale.

This is even more plausible if one considers that the orbitals involved in $\pi \rightarrow \pi^*$ back-bonding belong to cobalt. Thus, the overlap of such orbitals with the π^* of CO is not enough to influence the energy of the electrons of the metal core since the metal is from the first transition series. This is different if the metal core is formed by Rh or Ir atoms.

The substitution of two CO by a dppa makes the metal core more electron-rich and the reduction of the cluster becomes more difficult, as shown by the negative shift in $E^{0\prime}_{red}$. This argument is supported by the fact that a further substitution of two CO by another dppa (yielding **C**) gives rise to an almost equivalent negative shift in $E^{0\prime}_{red}$.

As for the second oxidation of **A** and the first oxidation of **B** and **C**, they appear in the three clusters at around 1.7 eV with respect to the first reduction. Thus, the MO involved in the oxidation cannot be the HOMO, which is *ca.* 1.3 eV from the LUMO [24]. This MO should be $20a_1$, the closest in energy to the potential at which electrochemical oxidation takes place. The small energy difference could be due to the overpotential necessary for the electron transfer to take place. This oxidation should correspond to the electron transfer $(20a_1)^2 \rightarrow (20a_1)^1$.

In order to explain why electrons occupying the HOMO of the clusters, a MO with higher energy and thus theoretically more easily oxidable than $20a_1$, do not participate in electron-transfer, it is necessary to remember that the kinetics of this process are also a function of the MO symmetry. In this case, the HOMO symmetry does not favour electron-transfers to the electrode. The HOMO is a metal-centred MO of the metal core, "protected" from the electrode by the ligands. The ligands could exert a shielding effect, impeding the electron transfers. Table 4 summarizes all the above conclusions.

[Co$_4$(CO)$_{12}$] shows an oxidation peak at 1.05 V/SCE, of small intensity and without a corresponding reduction peak, which grows with time. The shape of this wave is typical of the irreversible oxidation of an adsorbed substance. The MO diagram in Fig. 5 indicates that the corresponding electrochemical transition should be attributed to electron-transfers between the HOMO of the compound and the electrode, since this orbital is at around -1.3 eV from the LUMO, a value very close to the separation between this oxidation peak and the first reduction of the cluster. Thus, it seems that when the electron transfer takes place from species in the outer Helmholtz plane (OHP), not specifically adsorbed, the MO involved in the oxidation is $20a_1$. However, when the compound is adsorbed, *i.e.* in the inner Helmholtz plane (IHP), closer interaction between the electrons of the HOMO and the dangling bonds of the electrode surface atoms facilitates electron-transfer from it to the electrode, which explains the adsorption peak at 1.05 V/SCE.

The dppa-substituted compounds do not show any indication of a similar peak in the recorded voltammograms and so it seems likely that the dppa ligands impede adsorption of the cluster molecule on the elec-

trode surface. In this case only an oxidation from the OHP with participation of electrons from $20a_1$ can take place, giving rise to the main oxidation peak.

3. Experimental details

All manipulations were carried out by standard Schlenk techniques under oxygen-free N_2. Dichloroethane (DCE) was dried over, and distilled from, P_4O_{10}. Deuterated chloroform was degassed and stored over a Type 4Å molecular sieve.

The reagents $[Co_4(CO)_{12}]$ [9] and dppa [26] were prepared according to the literature and characterized by their IR and, in the case of dppa, NMR spectra.

The cobalt was determined by titration of the Co-EDTA complex in the presence of Eriochrome Black T as indicator. The microanalyses were performed by the Microanalytical Laboratory of this Department.

The IR spectra were recorded in the range 4000–200 cm^{-1} on a Nicolet 5DX FT-IR spectrometer using KBr plates and DCE solution. ^1H and ^{31}P NMR spectra were obtained on a Bruker WH-200-SY instrument. All ^1H NMR chemical shifts are relative to internal TMS, and ^{31}P shifts are relative to 85% aqueous H_3PO_4. The visible spectra were recorded on a Pye Unicam SP 8-100 ultraviolet spectrophotometer, using DCE as solvent.

Electrochemical measurements were made with a PAR Mo. 273 electrochemistry system and a 7047 A Hewlett Packard X-Y recorder. All experiments were carried out in a three electrode cell under dinitrogen in anhydrous deoxygenated solvent. The temperature of the solution was maintained at 25°C. Cyclic voltammetry studies were made on a platinum working electrode (0.15 cm^2 real surface area, as calculated in a separate experiment through the H-adatom charge in 0.5 M H_2SO_4 solution [27]) in DCE containing 0.1 M tetrabutylammonium perchlorate (TBAP) as supporting electrolyte. In a typical experiment, solutions were 5×10^{-4} M in cluster compound. A Pt gauze and a saturated calomel electrode (SCE) electrically connected to the study solution by a bridge filled with DCE + 0.1 M TBAP ending in a Luggin capillary were employed as auxiliary and reference electrodes, respectively. The ferricenium/ferrocene couple was measured under the same conditions to allow corrections for junction potentials ($E^{0\prime} = (E_{pa} + E_{pc})/2 = +0.495$ V) [28]. The stability potential window of the solvent was from +1.8 V to −2.0 V/SCE. Dppa was not reduced under our experimental conditions in the potential range at which the work was done, but showed an irreversible oxidation with $E_p = +1.2$ V/SCE at $v = 0.1$ V s^{-1}.

3.1. Preparation of $[Co_4(CO)_{10}(dppa)]$

To a solution of $[Co_4(CO)_{12}]$ (1 g, 1.75 mmol) in DCE in a dinitrogen-filled Schlenk flask, another solution of dppa (0.67 g, 1.75 mmol) in the same solvent was added. The mixture was stirred at room temperature and the progress of the reaction monitored by IR spectroscopy. After *ca.* 2 h the reaction was complete. The solution was filtered, concentrated and then chromatographed under N_2 on alumina with DCE/hexane (1:1). The neutral alumina (Merck) was previously treated under vacuum at 300°C during 2 h, then cooled under N_2 and deactivated with 10%, by weight, of N_2-saturated water. The brown band was concentrated under vacuum and cooled to −5°C giving brown crystals which were filtered off, washed with cold hexane and dried under vacuum. The yield was 1.24 g (79%). Anal. Found: C, 45.36; H, 2.44; N, 1.60; Co, 25.94. $C_{34}H_{21}Co_4NO_{10}P_2$ calcd.: C, 45.28; H, 2.33; N, 1.55; Co, 26.16%. ^1H NMR ($CDCl_3$): δ 3.21 (s, br, 1H, NH); 7.44 (*m*, *m*- and *p*-H, 12H); 7.78 (*m*, *o*-H, 8H). ^{31}P NMR ($CDCl_3$): δ 74.1 (s, br, coordinated P).

3.2. Preparation of $Co_4(CO)_8(dppa)_2$

By a similar procedure, heating at 40°C during 4 h, a DCE solution of $[Co_4(CO)_{12}]$ and dppa in a 1:2 ratio resulted in a green solution from which, following the steps described above, a green solid was obtained. Recrystallization from benzene/pentane (1:1) gave green crystals. The yield was 78%.

This complex is also obtained from $[Co_4(CO)_{10}(dppa)]$ and dppa in a 1:1 ratio, following the same procedure.

Anal. Found: C, 54.36; H, 3.52; N, 2.33; Co, 18.96. $C_{56}H_{42}Co_4N_2O_8P_4$ calcd.: C, 54.61; H, 3.41; N, 2.27; Co, 19.16%. ^1H NMR ($CDCl_3$): δ 3.63 (s, br, 2H, NH); 7.34 (*m*, *m*- and *p*-H, 24H); 7.45 (*m*, *o*-H, 16H). ^{31}P NMR ($CDCl_3$): δ 74.2 (s, br, coordinated P).

Acknowledgements

M.L.M. and J.G.V. wish to thank the DGICyT for part of the financial support of this work (grant no. MAT 90/0273). We thank Dr. Jesús H. Rodriguez Ramos for the ^{31}P NMR spectra.

References

1 D. J. Darensbourg and M. T. Incorvia, *Inorg. Chem., 19* (1980) 258.
2 D. J. Darensbourg and M. T. Incorvia, *Inorg. Chem., 20* (1981) 191.
3 D. J. Darensbourg, B. S. Peterson and R. E. Schmidt, *Organometallics, 1* (1982) 306.
4 D. J. Darensbourg, D. J. Zalewski, A. L. Rheingold and R. I. Durney, *Inorg. Chem., 25* (1986) 3281.

5 D. J. Darensbourg and B. J. Baldwin-Zuschke, *J. Am. Chem. Soc., 104* (1982) 3906.
6 G. F. Holland, D. E. Ellis and W. C. Trogler, *J. Am. Chem. Soc., 108* (1986) 1884.
7 J. Q. Wang, J. K. Shen, Y. C. Gao, Q. Z. Shi and F. Basolo, *J. Organomet. Chem., 417* (1991) 131.
8 J. R. Kennedy, P. Selz, A. L. Rheingold, W. C. Trogler and F. Basolo, *J. Am. Chem. Soc., 111* (1989) 3615.
9 R. Huq and A. Poë, *J. Organomet. Chem., 226* (1982) 277.
10 C. Moreno, M. J. Macazaga and S. Delgado, *J. Organomet. Chem., 407* (1991) 125.
11 M. G. Richmond and J. K. Kochi, *Inorg. Chem., 25* (1986) 656.
12 J. Rimmelin, R. Jund, M. Gross and A. Bahsoun, *J. Chem. Soc. Dalton Trans.*, (1990) 3189.
13 J. Rimmelin, P. Lemoine, M. Gross and D. de Montauzon, *Nouv. J. Chim., 7* (1983) 453.
14 J. Rimmelin, P. Lemoine, M. Gross, A. Bahsoun and J. A. Osborn, *Nouv. J. Chim., 9* (1985) 181.
15 A. A. Bahsoun, J. A. Osborn, C. Voelker, J. J. Bonnet and G. Lavigne, *Organometallics, 1* (1982) 1114.
16 D. Labroue and R. Poilblanc, *Inorg. Chim. Acta, 6* (1972) 387.
17 F. H. Carre, F. A. Cotton and B. A. Frenz, *Inorg. Chem., 15* (1976) 381.
18 (a) J. Ellermann, N. Geheeb, G. Zoubek and G. Huele, *Z. Naturforsch., Teil B, 32* (1977) 1271; (b) R. Usón, J. Fornies, R. Navarro and J. F. Cebollada, *J. Organomet. Chem., 304* (1986) 381.
19 A. J. Bard and L. R. Faulkner, *Electrochemical Methods*, Wiley, New York, 1980.
20 H. Scholl and K. Sochaj, *Electrochim. Acta, 36* (1991) 689.
21 P. Walden, H. Ulich and G. Busch, *Z. Phys. Chem., 123* (1926) 429.
22 Y. Mugnier, P. Reeb, C. Moise and E. Laviron, *J. Organomet. Chem., 254* (1983) 111.
23 C. Moreno, M. J. Macazaga and S. Delgado, *J. Organomet. Chem., 415* (1991) 271.
24 G. F. Holland, D. E. Ellis, D. R. Tyler, H. B. Gray and W. C. Trogler, *J. Am. Chem. Soc., 109* (1987) 4276.
25 R. Gomer and G. Tryson, *J. Chem. Phys., 66* (1977) 4413.
26 H. Nöth and L. Mainel, *Z. Anorg. Allg. Chem., 349* (1967) 225.
27 R. Woods, in A. J. Bard (ed.), *Electroanalytical Chemistry*, Vol. 9, New York, 1976.
28 G. Gritzner and J. Kuta, *Pure Appl. Chem., 54* (1982) 1527.